



Rotational paper-based electrochemiluminescence immunodevices for sensitive and multiplexed detection of cancer biomarkers

Xiange Sun^{a, c}, Bowei Li^{a, *}, Chunyuan Tian^b, Fabiao Yu^a, Na Zhou^a, Yinghua Zhan^d, Lingxin Chen^{a, **}

^a Key Laboratory of Coastal Environmental Processes and Ecological Remediation, Yantai Institute of Coastal Zone Research, Chinese Academy of Sciences, Yantai 264003, China

^b College of Chemistry and Chemical Engineering, Yantai University, Yantai 264005, China

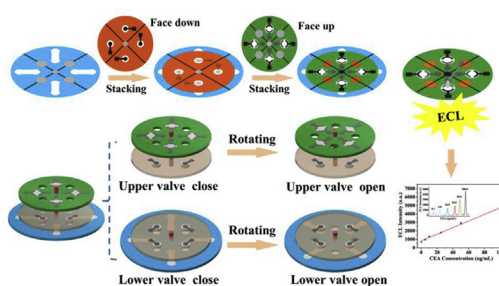
^c University of Chinese Academy of Sciences, Beijing 100049, China

^d Yantai Xinhua Health Outpatient Department, Yantai 264003, China

HIGHLIGHTS

- The novel rotational paper-based devices (RPADs) opened a new avenue for the fabrication of 3D paper-based devices.
- The integrated paper-based rotational valves could be easily operated in a simple, low-cost and user-friendly way.
- Multi-step ECL immunoassays were conducted for the detection of cancer biomarkers by the manipulation of rotational valves.

GRAPHICAL ABSTRACT



ARTICLE INFO

Article history:

Received 10 July 2017

Received in revised form

1 November 2017

Accepted 6 December 2017

Available online 27 December 2017

Keywords:

Microfluidic paper-based device
Electrochemiluminescence immunoassay
Valve
Cancer biomarker
Point-of-care

ABSTRACT

This paper describes a novel rotational paper-based analytical device (RPAD) to implement multi-step electrochemiluminescence (ECL) immunoassays. The integrated paper-based rotational valves can be easily controlled by rotating paper discs manually and this advantage makes it user-friendly to untrained users to carry out the multi-step assays. In addition, the rotational valves are reusable and the response time can be shortened to several seconds, which promotes the rotational paper-based device to have great advantages in multi-step operations. Under the control of rotational valves, multi-step ECL immunoassays were conducted on the rotational device for the multiplexed detection of carcinoembryonic antigen (CEA) and prostate specific antigen (PSA). The rotational device exhibited excellent analytical performance for CEA and PSA, and they could be detected in the linear ranges of 0.1–100 ng mL⁻¹ and 0.1–50 ng mL⁻¹ with detection limits down to 0.07 ng mL⁻¹ and 0.03 ng mL⁻¹, respectively, which were within the ranges of clinical concentrations. We hope this technique will open a new avenue for the fabrication of paper-based valves and provide potential application in clinical diagnostics.

© 2017 Elsevier B.V. All rights reserved.

1. Introduction

Since the concept of microfluidic paper-based analytical devices (μ PADs) was firstly proposed by Whitesides' group [1], μ PADs have attracted considerable attention owing to the

* Corresponding author.

** Corresponding author.

E-mail addresses: bwli@yic.ac.cn (B. Li), lxchen@yic.ac.cn (L. Chen).

advantages of low cost, simple operation, excellent biocompatibility and portability. In addition, driven by the development of biotechnology, nanotechnology and microfluidic technology, μ PADs have rapidly developed into a new analytical platform [2–7] for medical diagnostics, food safety as well as environmental monitoring. A variety of detection techniques have been applied to the development of versatile μ PADs, such as colorimetry [8–10], luminescence [11,12], electrochemical detection [13–16], fluorescence [17,18] and surface-enhanced Raman scattering [19,20]. Apart from these detection methods, electrochemiluminescence (ECL) detection that combined the advantages of luminescence and electrochemical detection was also integrated into paper-based sensors [21,22]. Due to the high sensitivity and wide dynamic range, paper-based ECL detection has been demonstrated for biological and chemical analysis [23–26]. For instance, Delaney et al. reported a ECL microfluidic paper-based sensor for the detection of 2-(dibutylamino)-ethanol (DBAE) and nicotinamide adenine dinucleotide [27], and Li et al. developed a simple 3D origami multiple ECL paper-based immunodevice for the sensitive detection of tumor markers using multi-labeled nanoporous gold-carbon spheres as tracers to amplify ECL signal [28].

The fluid flow within the μ PADs was driven by capillary forces rather than the complex pump system. However, this unique advantage brought some difficulties to the fluid control, which was challenging for the development of paper-based device with high analytical performance. Fortunately, several innovative valving strategies have been proposed to improve the flow-control capability of paper-based device [29–32]. Whitesides et al. integrated push-button valves into the 3D paper-based device in which the connection between vertical fluid channels was activated manually by pressing a ballpoint pen [33], and Fu et al. described a time-metered valve that actuated by an absorbent sponge [34]. However, these methods suffered from some restrictions such as tedious fabrication or only one-time use. Based on the change of the fluid velocity within a channel, some chemical reagents including dissolvable sucrose [32], paraffin wax [35] and surfactant [36] played the role of valves to delay or control the fluid flow. But the introductions of chemical reagents in this strategy maybe bring interference to the detection process. Therefore, it urgently needed to develop robust, user-friendly and reusable paper-based valves to meet the requirement of multi-step or complicated assays.

In this work, we developed a rotational paper-based ECL immunodevice for the sensitive and multiplexed detection of cancer biomarkers based on the integration of rotational valves. The rotational paper-based device was fabricated by assembling three designed paper discs together using a hollow rivet and the “On/Off” states of paper-based valves were easily controlled by the rotation of paper discs. Simple fabrication and easy operation of the rotational valves made it user-friendly to untrained users to conduct multi-step operations. Different from other valves that used only once, the rotational valves presented could be dried for reuse and had short response time. Based on the manipulation of rotational valves, multi-step ECL immunoassays were conducted on the rotational device, and immunoreaction processes and ECL detection were integrated into the rotational paper-based device successfully, which considerably improved the integration of paper-based device. Combined with tris-(bipyridine)-ruthenium (II) - tripropylamine ECL ($[\text{Ru}(\text{bpy})_3]^{2+}$ - TPA) detection system, the rotational paper-based device provided a new strategy for the simple, low-cost, rapid and portable immunoassay and exhibited excellent analytical performance for the quantitative analysis of cancer biomarkers.

2. Experimental section

2.1. Materials

Carcinoembryonic antigen (CEA), prostate specific antigen (PSA), capture antibody CEA and PSA, $[\text{Ru}(\text{bpy})_3]^{2+}$ -labeled signal antibody CEA and PSA were purchased from Shanghai Linc-Bio Science Co. Ltd. Carbon ink (ED423ss) was purchased from Acheson. Silver/silver chloride ink (CNC-01) was purchased from Xuzhou Bohui New Materials Tech. Co. Ltd (Jiangsu, China). Whatman No.1 chromatography paper (46 cm \times 57 cm) was obtained from GE Healthcare Worldwide Company (Pudong Shanghai, China) and was cut into A4 size for further use. Glutaraldehyde (GA), chitosan, bovine serum albumin (BSA) and tripropylamine (TPA) were purchased from Sigma-Aldrich. Carboxyl-functionalized multi-walled carbon nanotubes (MWCNTs) were purchased from Chengdu Organic Chemicals Co. Ltd. Serum samples were kindly provided by Yantai Xinhua Health Outpatient Department. All reagents were analytical grade and used without further purification. Ultrapure water ($>18.2 \text{ M}\Omega$) used for the whole experiment was obtained from a Millipore water purification system. Blocking buffer was 10 mM phosphate buffer solution (PBS, pH = 7.4) containing 0.5% bovine serum albumin (BSA), and washing buffer was 10 mM PBS (pH = 7.4) containing 0.05% Tween-20.

2.2. Instrumentation

The ECL signals were measured using MPI-E multifunctional electrochemical and chemiluminescent analytical system (Xi'an Remex Analytical Instrument Co. Ltd., China). The electrochemical impedance spectroscopy (EIS) was performed with a CHI 760E electrochemical workstation (Shanghai Chenhua Instruments Co., China). The paper-based device was fabricated using a commercial solid-wax printer (XEROX Phaser 8560DN, Japan).

2.3. Design and fabrication of the rotational paper-based device

The rotational paper-based device was designed with three paper discs, as shown in Fig. 1A. The detection disc (57 mm in diameter) contained four immunozones (white color, 6 mm in diameter) that screen-printed with carbon working electrodes. The auxiliary disc (57 mm in diameter) contained four punched holes (8 mm in diameter) and four hydrophilic zones (8 mm in diameter) on the surface of which the reference electrode and counter electrode were screen-printed. The three-electrode system could be constructed by rotating the auxiliary disc, and redox reaction could occur on the surface of the working electrode with the help of the reference electrode and counter electrode. The washing disc (70 mm in diameter) consisted of four punched holes (8 mm in diameter) and four washing channels that could connect to the immunozones vertically to carry out washing process through the rotation of the washing disc, as shown in Fig. 1C. Obviously, two black cross lines could be seen on three paper discs and this made it easier to identify the rotational position of paper discs. In addition, a rivet hole with a diameter of 3 mm was punched on each paper disc for the assembly of the rotational paper-based device.

The auxiliary disc, detection disc and washing disc within the rotational paper-based device were fabricated using wax-printing method and screen-printing technique, and the fabrication procedures were similar to our previous work [37]. Briefly, the patterns on paper discs were designed with Adobe Illustrator CS4 software and printed on chromatography paper using a commercial solid-wax printer. Then the paper sheet was placed in an oven at 150 °C for 30 s to melt the wax, which allowed wax to penetrate into the back of paper and form hydrophobic barriers. After the

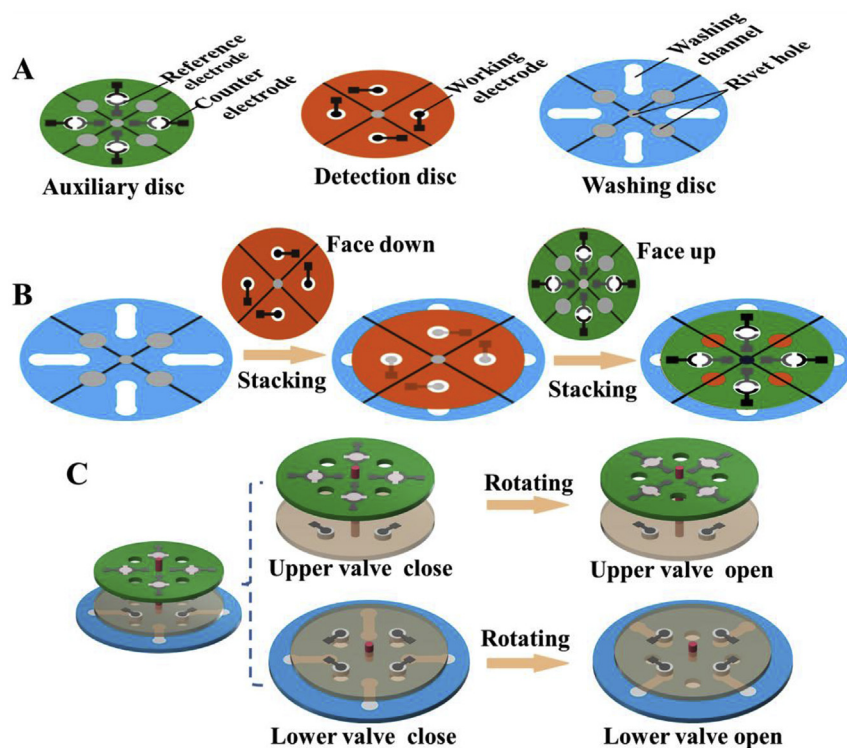


Fig. 1. (A) Design of three paper discs within the rotational paper-based device. Electrodes were integrated on the auxiliary disc and detection disc. (B) Fabrication procedures for the rotational paper-based device. (C) Integration of rotational valves on the rotational paper-based device. The “On/Off” states of upper valves were controlled by rotating the auxiliary disc, and the “On/Off” states of lower valves were controlled by rotating the washing disc.

paper sheet cooled to room temperature, the working electrode, counter electrode and reference electrode were screen-printed on the paper using carbon ink and silver/silver chloride ink, respectively, as shown in Fig. S1. After that, the paper sheet was cut into individual paper-based disc by a scissor and holes were punched on paper discs.

The rotational paper-based device was fabricated by assembling the auxiliary disc, detection disc and washing disc together, as shown in Fig. 1B and Movie S1. Firstly, the washing disc, detection disc and auxiliary disc were stacked together in sequence and the detection disc needed to be placed face-down. Then a hollow rivet passed through the rivet hole of three paper discs and was beaten with a hammer. After that, it could be found that the end of the rivet expanded about 1.5 times of the original size, which allowed the auxiliary disc, detection disc and washing disc to assemble together and obtain the rotational paper-based device.

Supplementary video related to this article can be found at <https://doi.org/10.1016/j.aca.2017.12.005>.

2.4. ECL immunoassays on the rotational device

ECL immunoassays were conducted on the rotational device for the multiplexed detection of CEA and PSA based on the manipulation of the rotational valves. As shown in Fig. 2A, the rotational valves were used to manipulate the multi-step ECL immunoassay processes. For the incubation process, the auxiliary disc was rotated to close the upper valves and expose four immunozones outside. Then the washing disc was also rotated to close the lower valves and disconnect the washing channel and the immunozones, as shown in Fig. S4A. After rotational valves were all closed, the reagent was added into the immunozones and carried out reaction. After the reaction process, the washing process was carried out and the washing disc was rotated to open the lower valves and connect

the washing channel and the immunozones, as displayed in Fig. S4B. With the aids of the clamps, the washing channels could contact the immunozones tightly and 30 μL of washing buffer was added to the immunozones to remove the unbound reagent relying on capillary forces. The paper-based rotational valves could be air dried for recovering the wicking ability and the immunozones were washed three times to reduce the nonspecific adsorption. Subsequently the washing disc was rotated again to disconnect the washing channel and the immunozones to carry out the next step incubation process. For the sandwich-type ECL immunoassay, immunoreaction processes mainly involved immobilization of capture antibody, nonspecific blocking, and incubations of antigen and signal antibody. Therefore, the incubation and washing operations in every step immunoreaction process could be carried out sequentially by rotating the washing disc.

The detailed multi-step ECL immunoassay procedures on the rotational device were displayed in Fig. 2B. Briefly, 5.0 μL of MWCNTs was added to the immunozones and dried at room temperature. Then 5.0 μL of 0.25 mg mL^{-1} chitosan was coated on the immunozones based on the static attraction between positively charged chitosan and negatively charged cellulose. Subsequently, 5.0 μL of 2.5% glutaraldehyde was used as cross-linker to immobilize capture antibody on the paper. After it reacted with chitosan, the washing disc was rotated for washing. After that, 5.0 μL of CEA and PSA capture antibody (20 $\mu\text{g mL}^{-1}$) were applied to corresponding immunozones and reacted with glutaraldehyde for 40 min, respectively. After the excess antibodies were washed with washing buffer, the immunozones were blocked with 5.0 μL of 0.5% BSA solution for 15 min and washed. After that, 5.0 μL of CEA and PSA were added to corresponding immunozones, respectively, incubated and washed. Finally, 5.0 μL of 10 $\mu\text{g mL}^{-1}$ $[\text{Ru}(\text{bpy})_3]^{2+}$ -labeled signal antibody was added, and allowed to incubate at room temperature. After rotating the washing disc and washing with

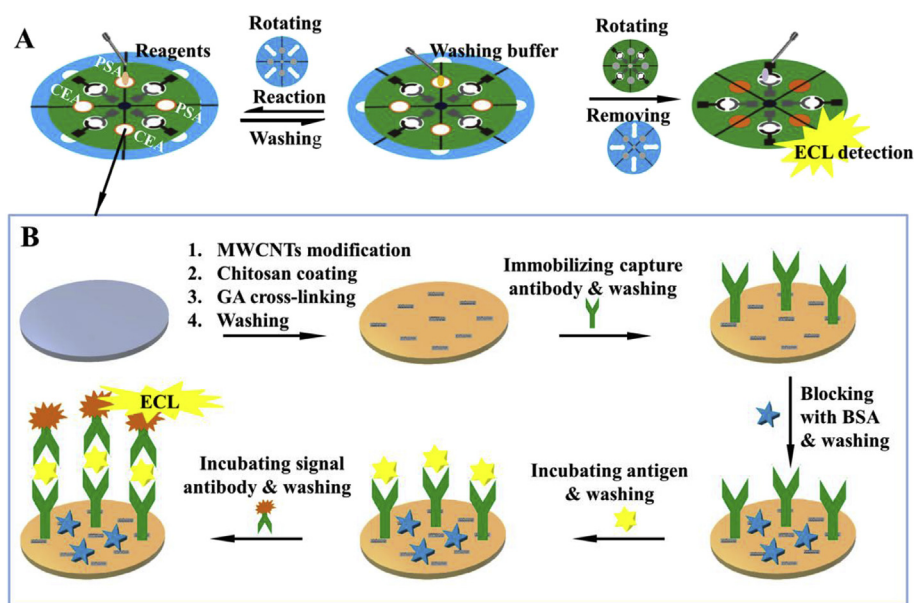


Fig. 2. Valve-controlled ECL immunoassay on the rotational device. (A) Multi-step ECL immunoassay was controlled by the rotational valves. The incubation and washing processes were controlled by rotating the washing disc, and ECL detection was conducted after the rotation of auxiliary disc and removal of the washing disc. (B) ECL immunoassay procedure on the rotational device.

washing buffer, sandwich ECL immunoreactions were established on the rotational device.

For the ECL detection process, firstly the washing disc was removed from the rotational device, and then the auxiliary disc was rotated to open the upper valves. The rotation of auxiliary disc allowed the construction of four three-electrode systems on the rotational device. With the help of home-made device, the auxiliary disc could contact the detection disc tightly. The electrochemical detection was carried out after 40 μL of PBS solution containing 10 mM tripropylamine (TPA) and 0.1 M KCl was added to the electrochemical cell. The ECL intensity was measured in the potential range from 0.5 to 1.2 V at a scan rate of 100 mV s^{-1} and a photomultiplier tube voltage of 800 V.

3. Results and discussion

3.1. Fabrication of the rotational device

In this work, a new strategy was proposed to control fluid flow and implement multi-step ECL immunoassay based on the integration of the rotational valves on the paper-based device. The rotational device was fabricated easily by assembling three paper discs together using a hollow rivet, as shown in Movie S1. Compared with the fabrication method of 3D μPADs that glued paper-based chips together using the double-sided adhesive tape [33], it could be found that our fabrication method did not require the tedious alignment steps and the whole fabrication procedures was greatly simplified. Besides, the simple, low-cost and rapid fabrication of the paper-based device was achieved through the combination of wax-printing method and screen-printing technique.

Significantly, the auxiliary disc, detection disc and washing disc could be rotated around the rivet independently so that the rotational valves were integrated into the paper-based device successfully. The fundamental mechanism of the rotational valve utilized here was that the rotation of the channel on one paper disc caused the connection or disconnection with the channel on the other paper disc, and Fig. 1C illustrated the integration of rotational

valves on the rotational paper-based device. The upper four valves consisted of the auxiliary disc and detection disc, and the “On/Off” states could be controlled by rotating the auxiliary disc. Similarly, the lower four valves were composed of the detection disc and washing disc, and the “On/Off” states could be controlled by rotating the washing disc. Under the control of the upper valve and lower valve, multi-step ECL immunoassay mainly including incubation, washing and detection processes was conducted sequentially on the rotational device. It could be found that the rotational valves were easy to operate, and it just needed to rotate the auxiliary disc and the washing disc manually. What’s more, the valves were reusable and the response time could be shortened to several seconds. Therefore, the integration of rotational valves provided a relatively simple, robust and user-friendly strategy for the multi-step immunoassay compared with the literature [38,39].

3.2. Characterization of ECL immunoassay

To confirm the success of ECL immunoassay on the proposed rotational device, electrochemical impedance spectroscopy (EIS) was used to characterize immunoreaction process in 5.0 mM $[\text{Fe}(\text{CN})_6]^{3-/4-}$ containing 0.1 M KCl, as shown in Fig. 3. It could be found that the bare working electrode had a relatively low resistance (Fig. 3, curve a). After the modification of MWCNTs, the resistance decreased significantly (Fig. 3, curve b) on account of the excellent conductivity of MWCNTs. Then a further decrease (Fig. 3, curve c) was observed after the chitosan was coated. This could be explained that the electrostatic attraction between the positively charged amino group of chitosan and negatively charged $[\text{Fe}(\text{CN})_6]^{3-/4-}$ accelerated electron transfer on the electrode surface. In contrast, the cross-linking of glutaraldehyde subsequently reduced amount of amino group and resulted in remarkable increase of resistance (Fig. 3, curve d). It was also observed that the resistance further increased gradually (Fig. 3, curve e, f, g and h) with sequential incubations of capture antibody, BSA, antigen and signal antibody. The possible reason was that the diffusion of $[\text{Fe}(\text{CN})_6]^{3-/4-}$ toward the sensing interface was greatly hindered by the non-conducting protein layer on the electrode surface. The

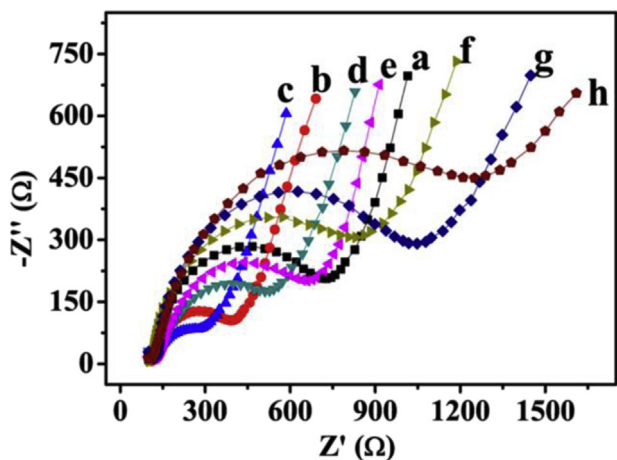


Fig. 3. Electrochemical impedance spectroscopy (EIS) of immunoassay procedure: (a) bare working electrode; (b) MWCNTs modified working electrode; (c) chitosan/MWCNTs modified working electrode; (d) glutaraldehyde/chitosan/MWCNTs modified working electrode; (e) anti-CEA/glutaraldehyde/chitosan/MWCNTs modified working electrode; (f) after blocking with BSA; (g) incubation with CEA; (h) incubation with signal antibody CEA.

differences of resistance between every step reaction reflected the changes of electrode surface, which indicated successful modifications of MWCNTs, chitosan, glutaraldehyde, capture antibody, BSA, antigen and signal antibody on the rotational paper-based device. In addition, other characterizations such as cyclic voltammetry (CV) and scan electron microscopy were also conducted to demonstrate the success of immunoassay on the rotational device (details could be found in the Supporting Information).

3.3. ECL emission on the rotational device

The ECL emission behaviors were also studied to demonstrate the feasibility of the rotational paper-based device. Using CEA as a model, ECL responses of signal antibody/antigen/BSA/anti-CEA/GA/chitosan/MWCNTs/working electrode in the presence of TPA were displayed in Fig. 4A. The ECL peak intensity appeared approximately at 1.15 V in the anodic process due to the generation of $[\text{Ru}(\text{bpy})_3^*]^{2+}$ that was formed by the redox reaction between $[\text{Ru}(\text{bpy})_3]^{2+}$ and TPA on the electrode surface. To verify the signal amplification of MWCNTs, the capture antibody was coupled to the

electrode surface without the modification of MWCNTs and a comparatively lower ECL intensity was obtained (Fig. 4A, curve b), which suggested the presence of MWCNTs could accelerate electron transfer and amplify ECL intensity. Also it could be found that the ECL intensity in the presence of CEA (Fig. 4A, curve c) was much higher than that in the absence of CEA (Fig. 4A, curve a), which revealed the immunoreaction had low nonspecific adsorption of $[\text{Ru}(\text{bpy})_3]^{2+}$ -labeled signal antibody. What's more, the fact that the ECL intensity increased with the increasing concentration of CEA (Fig. 4A, curve d) further confirmed the rotational ECL immuno-device could be used for the determination of antigens. Fig. 4B showed the ECL responses for 15 cycles of continuous potential scans from 0.5 to 1.2 V at a CEA concentration of 50 ng mL^{-1} . Stable ECL signals were observed obviously and relative standard deviation (RSD) between ECL intensities was only 1.48%, which illustrated the ECL intensity had good stability on the rotational device.

3.4. Optimization of experimental conditions

Since pH had great influence on electrochemical immunoassay, the effect of solution acidity on ECL response was investigated. In the $[\text{Ru}(\text{bpy})_3]^{2+}$ -TPA ECL detection system, the solubility of TPA was closely related to the acidity of the solution. As shown in Fig. 5A, ECL intensity increased as pH value increased gradually from 6.0 to 7.4 and then decreased. The ECL intensity for CEA and PSA reached the maximum at pH 7.4. Thus, pH 7.4 was the most suitable condition for ECL detection and was selected for the further study.

The incubation time was also a critical parameter affecting the ECL intensity. As shown in Fig. 5B, with the increase of antigen incubation time, ECL intensities for 50 ng mL^{-1} CEA and 25 ng mL^{-1} PSA increased gradually and then reached a plateau, which revealed that immunoreaction between antigen and capture antibody was almost complete. The short diffusion distance of antigen was beneficial to shorten the antigen incubation time on the paper-based device [4]. As the ECL intensity reached stable, the time for CEA and PSA were 240 s and 210 s, respectively. To be convenient for the simultaneous detection of CEA and PSA on the rotational device, 240 s was chosen as the optimal antigen incubation time, and the result was consistent with previous reports [40,41].

3.5. Analytical performance of the rotational device

Under the optimum conditions, CEA and PSA standard solution

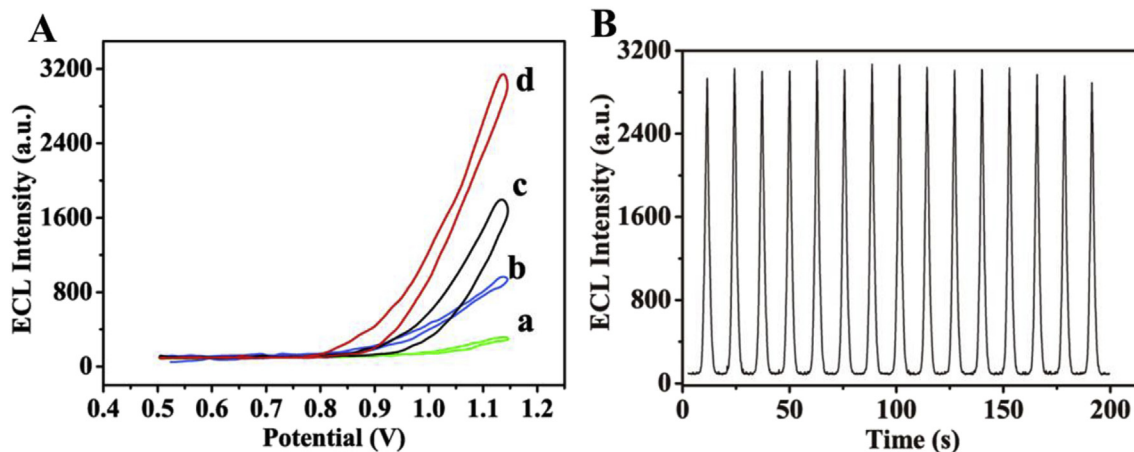


Fig. 4. (A) ECL-potential curves obtained from (a) background without antigen; (b) immunoreaction with 50 ng mL^{-1} CEA in the absence of MWCNTs; immunoreaction with (c) 25 ng mL^{-1} CEA and (d) 50 ng mL^{-1} CEA after the modification of MWCNTs, respectively. (B) ECL emission at a CEA concentration of 50 ng mL^{-1} on the rotational device.

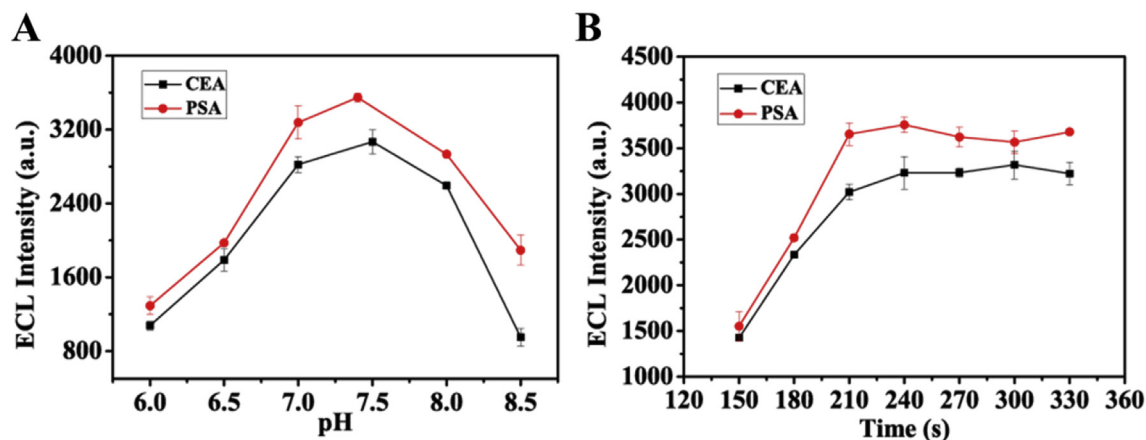


Fig. 5. (A) Effect of pH on ECL intensity. (B) Effect of incubation time on ECL intensity. 50 ng mL⁻¹ CEA and 25 ng mL⁻¹ PSA were used in the optimization of experimental conditions.

at various concentrations were applied to immunozones to verify the analytical performance of the rotational device, and Fig. 6 showed the ECL responses and linear calibration curves for two cancer biomarkers. It could be found that good linear relationships between ECL intensity and concentration were established with wide dynamic ranges. The linear regression equations obtained for CEA and PSA were $I_{CEA} = 39.15 C_{CEA} (\text{ng mL}^{-1}) + 825.0$ ($R^2 = 0.993$) and $I_{PSA} = 115.34 C_{PSA} (\text{ng mL}^{-1}) + 613.4$ ($R^2 = 0.995$) with the linear ranges of 0.1–100 ng mL⁻¹ and 0.1–50 ng mL⁻¹, respectively. The detection limits at a signal-to-noise ratio of 3 could be found to be 0.07 ng mL⁻¹ and 0.03 ng mL⁻¹, respectively. Because the cutoff values of CEA and PSA in clinical diagnosis were 5 ng mL⁻¹ and 4 ng mL⁻¹ [42,43], respectively, the obtained linear curves had potential in the determination of CEA and PSA in serum samples.

To verify the feasibility of proposed rotational paper-based ECL immunodevices in real biological samples, the determination of CEA and PSA in real human serum was conducted on the rotational device. And the results were compared with that obtained from Yantai Xinhua Health Outpatient Department using the chemiluminescence method. As displayed in Table 1, the results of two methods were in agreement within the relative error range from -8% to 7.5%, which suggested that the rotational paper-based ECL devices had a strong potential to become a low-cost, user-friendly and sensitive diagnostic platform for the determination of CEA and PSA in real samples.

Table 1

Assay results of human serum samples. (n = 3).

| Analytes | CEA (ng mL ⁻¹) | | | PSA (ng mL ⁻¹) | |
|--------------------|----------------------------|-----------|-----------|----------------------------|-----------|
| | Sample 1 | Sample 2 | Sample 3 | Sample 1 | Sample 2 |
| Proposed method | 14.6 ± 0.7 | 4.3 ± 0.2 | 2.3 ± 0.3 | 0.55 ± 0.1 | 1.3 ± 0.2 |
| Reference method | 14.9 | 4.0 | 2.5 | 0.53 | 1.36 |
| Relative error (%) | -2.01 | 7.50 | -8.00 | 3.77 | -4.41 |

4. Conclusions

This work was the first demonstration of the integration of rotational valves into the microfluidic paper-based ECL immunodevice for the sensitive and multiplexed detection of cancer biomarkers. The cleverly designed paper-based device allowed paper discs to rotate around the center so that rotational valves were integrated into the paper-based device successfully and their "On/Off" states could be easily controlled by rotating the paper discs. The repeated use and short response time could be obtained in the operation processes, which made the rotational paper-based device have great advantages in multi-step operations. The functions of rotational valves were demonstrated by carrying out multistep ECL immunoassay and the device exhibited excellent analytical performance for the quantitative analysis of cancer biomarkers with low detection limits. In addition, there was considerable scope for

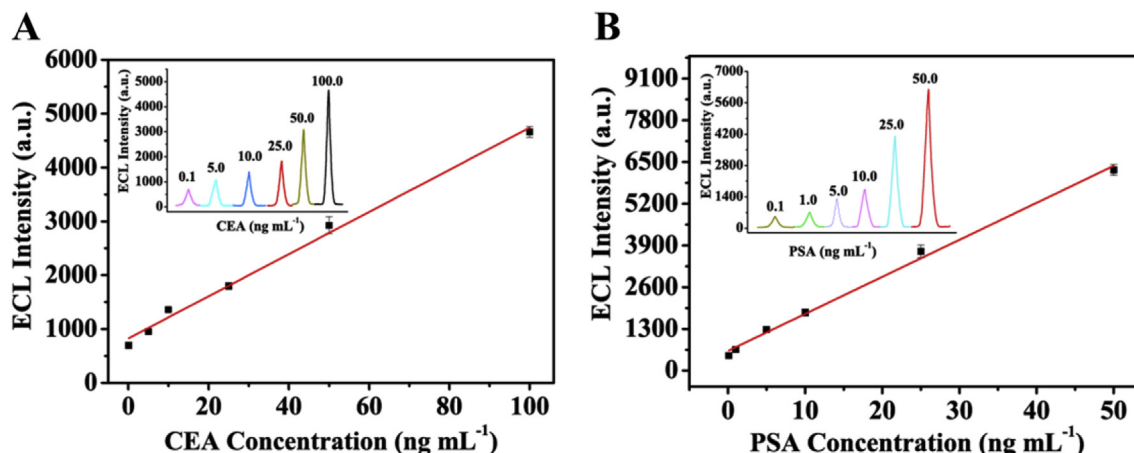


Fig. 6. Calibration curves for (A) CEA and (B) PSA on the rotational device (n = 3). Inset: ECL intensities with different concentrations of cancer biomarkers.

further improving detection limits and sensitivities with various signal amplification strategies, such as the assistance of enzyme and the incorporation of nanomaterials. Due to high integration and easy operation, the rotational paper-based ECL immunodevices were expected to be a rapid, low-cost and sensitive analytical platform for point-of-care testing.

Acknowledgements

This work was financially supported by the National Natural Science Foundation of China (Grant No. 41776110, 21205131 and 21775162), the Science and Technology Development Plan of Yantai (Grant No. 2015ZH087), the National Key Research and Development Program of China (Grant No. 2016YFC1400702), and the Project Sponsored by the Scientific Research Foundation for the Returned Overseas Chinese Scholars, State Education Ministry.

Appendix A. Supplementary data

Supplementary data related to this article can be found at <https://doi.org/10.1016/j.aca.2017.12.005>.

References

- [1] A.W. Martinez, S.T. Phillips, M.J. Butte, G.M. Whitesides, Patterned paper as a platform for inexpensive, low-volume, portable bioassays, *Angew. Chem. Int. Ed.* 46 (2007) 1318–1320.
- [2] A.M. Lopez-Marzo, A. Merkoci, Paper-based sensors and assays: a success of the engineering design and the convergence of knowledge areas, *Lab Chip* 16 (2016) 3150–3176.
- [3] K.F. Lei, C.H. Huang, R.L. Kuo, C.K. Chang, K.F. Chen, K.C. Tsao, N.M. Tsang, Paper-based enzyme-free immunoassay for rapid detection and subtyping of influenza A H1N1 and H3N2 viruses, *Anal. Chim. Acta* 883 (2015) 37–44.
- [4] C.M. Cheng, A.W. Martinez, J. Gong, C.R. Mace, S.T. Phillips, E. Carrilho, K.A. Mirica, G.M. Whitesides, Paper-based ELISA, *Angew. Chem. Int. Ed.* 49 (2010) 4771–4774.
- [5] B. Xu, Y. Du, J. Lin, M. Qi, B. Shu, X. Wen, G. Liang, B. Chen, D. Liu, Simultaneous identification and antimicrobial susceptibility testing of multiple uropathogens on a microfluidic chip with paper-supported cell culture arrays, *Anal. Chem.* 88 (2016) 11593–11600.
- [6] H. Wang, Y.J. Li, J.F. Wei, J.R. Xu, Y.H. Wang, G.X. Zheng, Paper-based three-dimensional microfluidic device for monitoring of heavy metals with a camera cell phone, *Anal. Bioanal. Chem.* 406 (2014) 2799–2807.
- [7] N.A. Meredith, C. Quinn, D.M. Cate, T.H. Reilly, J. Volckens, C.S. Henry, Paper-based analytical devices for environmental analysis, *Analyst* 141 (2016) 1874–1887.
- [8] R.A.G. de Oliveira, F. Camargo, N.C. Pesquero, R.C. Faria, A simple method to produce 2D and 3D microfluidic paper-based analytical devices for clinical analysis, *Anal. Chim. Acta* 957 (2017) 40–46.
- [9] P. Teengam, W. Siangproh, A. Tuantranont, T. Vilaivan, O. Chailapakul, C.S. Henry, Multiplex paper-based colorimetric DNA sensor using pyrrolidinyl peptide nucleic acid-induced AgNPs aggregation for detecting MERS-CoV, MTB, and HPV oligonucleotides, *Anal. Chem.* 89 (2017) 5428–5435.
- [10] S. Chaiyo, W. Siangproh, A. Apilux, O. Chailapakul, Highly selective and sensitive paper-based colorimetric sensor using thiosulfate catalytic etching of silver nanoparticles for trace determination of copper ions, *Anal. Chim. Acta* 866 (2015) 75–83.
- [11] J. Yu, L. Ge, J. Huang, S. Wang, S. Ge, Microfluidic paper-based chemiluminescence biosensor for simultaneous determination of glucose and uric acid, *Lab Chip* 11 (2011) 1286–1291.
- [12] W. Liu, C.L. Cassano, X. Xu, Z.H. Fan, Laminated paper-based analytical devices (LPAD) with origami-enabled chemiluminescence immunoassay for cotinine detection in mouse serum, *Anal. Chem.* 85 (2013) 10270–10276.
- [13] A.C. Glavan, D.C. Christodouleas, B. Mosadegh, H.D. Yu, B.S. Smith, J. Lessing, M.T. Fernandez-Abedul, G.M. Whitesides, Folding analytical devices for electrochemical ELISA in hydrophobic R-H paper, *Anal. Chem.* 86 (2014) 11999–12007.
- [14] M. Su, L. Ge, S. Ge, N. Li, J. Yu, M. Yan, J. Huang, Paper-based electrochemical cyto-device for sensitive detection of cancer cells and in situ anticancer drug screening, *Anal. Chim. Acta* 847 (2014) 1–9.
- [15] J. Ding, B. Li, L. Chen, W. Qin, A three-dimensional origami paper-based device for potentiometric biosensing, *Angew. Chem. Int. Ed.* 55 (2016) 13033–13037.
- [16] J.M. Oh, K.F. Chow, Recent developments in electrochemical paper-based analytical devices, *Anal. Methods* 7 (2015) 7951–7960.
- [17] J. Qi, B. Li, X. Wang, Z. Zhang, Z. Wang, J. Han, L. Chen, Three-dimensional paper-based microfluidic chip device for multiplexed fluorescence detection of Cu^{2+} and Hg^{2+} ions based on ion, imprinting technology, *Sens. Actuators B: Chem.* 251 (2017) 224–233.
- [18] B. Li, Z. Zhang, J. Qi, N. Zhou, S. Qin, J. Choo, L. Chen, Quantum dot-based molecularly imprinted polymers on three-dimensional origami paper microfluidic chip for fluorescence detection of phycoerythrin, *ACS Sens* 2 (2017) 243–250.
- [19] B. Li, W. Zhang, L. Chen, B. Lin, A fast and low-cost spray method for prototyping and depositing surface-enhanced Raman scattering arrays on microfluidic paper based device, *Electrophoresis* 34 (2013) 2162–2168.
- [20] W. Zhang, B. Li, L. Chen, Y. Wang, D. Gao, X. Ma, A. Wu, Brushing, a simple way to fabricate SERS active paper substrates, *Anal. Methods* 6 (2014) 2066–2071.
- [21] Y. Zhang, W. Liu, S. Ge, M. Yan, S. Wang, J. Yu, N. Li, X. Song, Multiplexed sandwich immunoassays using flow-injection electrochemiluminescence with designed substrate spatial-resolved technique for detection of tumor markers, *Biosens. Bioelectron.* 41 (2013) 684–690.
- [22] S. Wang, L. Ge, Y. Zhang, X. Song, N. Li, S. Ge, J. Yu, Battery-triggered microfluidic paper-based multiplex electrochemiluminescence immunodevice based on potential-resolution strategy, *Lab Chip* 12 (2012) 4489–4498.
- [23] L. Ge, J. Yan, X. Song, M. Yan, S. Ge, J. Yu, Three-dimensional paper-based electrochemiluminescence immunodevice for multiplexed measurement of biomarkers and point-of-care testing, *Biomaterials* 33 (2012) 1024–1031.
- [24] Y. Zhang, W. Liu, S. Ge, M. Yan, S. Wang, J. Yu, N. Li, X. Song, Multiplexed sandwich immunoassays using flow-injection electrochemiluminescence with designed substrate spatial-resolved technique for detection of tumor markers, *Biosens. Bioelectron.* 41 (2013) 684–690.
- [25] S. Wang, L. Ge, Y. Zhang, X. Song, N. Li, S. Ge, J. Yu, Battery-triggered microfluidic paper-based multiplex electrochemiluminescence immunodevice based on potential-resolution strategy, *Lab Chip* 12 (2012) 4489–4498.
- [26] M. Su, H. Liu, S. Ge, N. Ren, L. Ding, J. Yu, X. Song, An electrochemiluminescence lab-on-paper device for sensitive detection of two antigens at the MCF-7 cell surface based on porous bimetallic AuPd nanoparticles, *RSC Adv* 6 (2016) 16500–16506.
- [27] J.L. Delaney, C.F. Hogan, J. Tian, W. Shen, Electrogenerated chemiluminescence detection in paper-based microfluidic sensors, *Anal. Chem.* 83 (2011) 1300–1306.
- [28] W. Li, L. Li, S. Ge, X. Song, L. Ge, M. Yan, J. Yu, A 3D origami multiple electrochemiluminescence immunodevice based on a porous silver-paper electrode and multi-labeled nanoporous gold-carbon spheres, *Chem. Commun.* 49 (2013) 7687–7689.
- [29] E. Fu, C. Downs, Progress in the development and integration of fluid flow control tools in paper microfluidics, *Lab Chip* 17 (2017) 614–628.
- [30] S. Byrnes, G. Thiessen, E. Fu, Progress in the development of paper-based diagnostics for low-resource point-of-care settings, *Bioanalysis* 5 (2013) 2821–2836.
- [31] A.K. Yetisen, M.S. Akram, C.R. Lowe, Paper-based microfluidic point-of-care diagnostic devices, *Lab Chip* 13 (2013) 2210–2251.
- [32] B. Lutz, T. Liang, E. Fu, S. Ramachandran, P. Kauffman, P. Yager, Dissolvable fluidic time delays for programming multi-step assays in instrument-free paper diagnostics, *Lab Chip* 13 (2013) 2840–2847.
- [33] A.W. Martinez, S.T. Phillips, Z. Nie, C.M. Cheng, E. Carrilho, B.J. Wiley, G.M. Whitesides, Programmable diagnostic devices made from paper and tape, *Lab Chip* 10 (2010) 2499–2504.
- [34] B.J. Toley, J.A. Wang, M. Gupta, J.R. Buser, L.K. Lafleur, B.R. Lutz, E. Fu, P. Yager, A versatile valving toolkit for automating fluidic operations in paper microfluidic devices, *Lab Chip* 15 (2015) 1432–1444.
- [35] H. Noh, S.T. Phillips, Metering the capillary-driven flow of fluids in paper-based microfluidic devices, *Anal. Chem.* 82 (2010) 4181–4187.
- [36] H. Chen, J. Cogswell, C. Anagnostopoulos, M. Faghri, A fluidic diode, valves, and a sequential-loading circuit fabricated on layered paper, *Lab Chip* 12 (2012) 2909–2913.
- [37] B. Li, L. Yu, J. Qi, L. Fu, P. Zhang, L. Chen, Controlling capillary-driven fluid transport in paper-based microfluidic devices using a movable valve, *Anal. Chem.* 89 (2017) 5707–5712.
- [38] T. Tian, X. Wei, S. Jia, R. Zhang, J. Li, Z. Zhu, H. Zhang, Y. Ma, Z. Lin, C.J. Yang, Integration of target responsive hydrogel with cascaded enzymatic reactions and microfluidic paper-based analytical devices for point-of-care testing, *Biosens. Bioelectron.* 77 (2016) 537–542.
- [39] W. Liu, Y. Guo, M. Zhao, H. Li, Z. Zhang, Ring-oven washing technique integrated paper-based immunodevice for sensitive detection of cancer biomarker, *Anal. Chem.* 87 (2015) 7951–7957.
- [40] Y. Wu, P. Xue, Y. Kang, K.M. Hui, Paper-based microfluidic electrochemical immunodevice integrated with nanobioprobes onto graphene film for ultra-sensitive multiplexed detection of cancer biomarkers, *Anal. Chem.* 85 (2013) 8661–8668.
- [41] D. Zang, L. Ge, M. Yan, X. Song, J. Yu, Electrochemical immunoassay on a 3D microfluidic paper-based device, *Chem. Commun.* 48 (2012) 4683–4685.
- [42] N. Laboria, A. Fragoso, W. Kemmer, D. Latta, O. Nilsson, M. Luz Botero, K. Drese, C.K. O'Sullivan, Amperometric immunosensor for carcinoembryonic antigen in colon cancer samples based on monolayers of dendritic bipodal scaffolds, *Anal. Chem.* 82 (2010) 1712–1719.
- [43] W. Li, M. Li, S. Ge, M. Yan, J. Huang, J. Yu, Battery-triggered ultrasensitive electrochemiluminescence detection on microfluidic paper-based immunodevice based on dual-signal amplification strategy, *Anal. Chim. Acta* 767 (2013) 66–74.